COMPARISON OF RECENT COOLING TECHNIQUES FOR ENHANCING THE PERFORMANCE OF PHOTOVOLTAIC CELLS

Aswin Karkadakattil[1], Arjun Kallath[2], Adithyan P [3], Adithya Dayal[4]

This manuscript is the author's corrected version of a paper previously published in the *International Journal of Scientific Development and Research (IJSDR)*. Only minor typographical corrections and precise clarifications to the wording describing the experimental duration and dates (20–29 April) have been made for accuracy and transparency. No changes have been made to the experimental data, data-averaging methodology, results, figures, or conclusions. The published version of record remains unchanged and is available at: https://doi.org/10.56975/ijsdr.v10i4.302395

Abstract

Solar energy is a clean, renewable, and widely available source of power that can be utilized through photovoltaic (PV) and photothermal technologies. However, the performance of PV panels is highly sensitive to operating temperature, with electrical efficiency decreasing as panel temperature rises under strong solar radiation. This makes effective thermal management essential for improving both the efficiency and long-term reliability of photovoltaic systems. In this study, a comparative experimental analysis of passive cooling techniques for PV panels is carried out to identify the most effective approach for temperature control and performance improvement. Three passive cooling configurations were investigated: phase change material (PCM) cooling, fin-based cooling, and a hybrid system combining PCM and fins. OM35 was selected as the PCM based on the ambient climatic conditions of the experimental site. Aluminium fins were employed as extended surfaces to enhance heat dissipation through conduction, convection, and radiation. The performance of each cooling method was evaluated in terms of panel temperature reduction, electrical power output, and conversion efficiency. The experimental results show that all passive cooling techniques improved the performance of the photovoltaic panel compared with the uncooled reference case. Among the tested configurations, the fin-cooled system delivered the best overall performance, achieving a maximum temperature reduction of 10.37 °C. The hybrid PCM–fin system and the standalone PCM system achieved temperature reductions of 5.5 °C and 4.4 °C, respectively. In addition to improving electrical output, passive cooling also reduced thermal stresses on the PV panels, which may help extend their operational lifespan. Overall, the findings indicate that passive cooling particularly fin-based cooling provides a simple, effective, and practical solution for enhancing the efficiency and durability of photovoltaic systems.

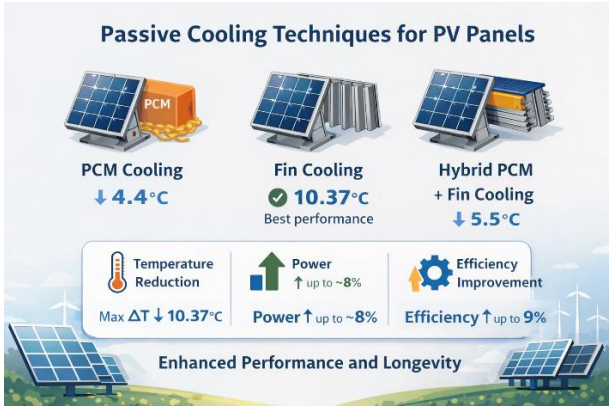

Keywords: Photovoltaic panel; Passive cooling; Phase change material; PCM; Fin cooling; Hybrid cooling; Thermal management; Solar energy; Efficiency enhancement; Temperature reduction; OM35

1. Introduction

Fossil fuels continue to dominate global energy production; however, their long-term availability is steadily diminishing. According to reports from the Millennium Alliance for Humanity and the Biosphere (MAHB), global reserves of oil, natural gas, and coal are expected to be exhausted by approximately 2052, 2060, and 2090, respectively. This projected depletion highlights the urgent need to transition toward sustainable and renewable energy sources. Renewable energy technologies including solar, wind, hydroelectric, geothermal, and biomass have therefore gained significant attention as viable alternatives for meeting future energy demands [1,2]. In addition to resource depletion, the extensive use of fossil fuels has resulted in severe environmental impacts, particularly due to greenhouse gas emissions that contribute to global climate change. Renewable energy systems, in contrast, generate electricity with minimal emissions during operation, thereby reducing carbon footprints and improving air quality [3]. Beyond environmental benefits, renewable energy also enhances energy security. Many countries rely heavily on imported fossil fuels, making their energy systems vulnerable to price volatility and geopolitical uncertainties. The utilization of locally available renewable resources can reduce this dependence and promote more resilient and self-sufficient energy infrastructures [4]. Among the various renewable energy options, solar energy stands out due to its abundance, versatility, and global availability. As a virtually inexhaustible resource, solar energy can be harnessed across diverse geographical regions. Currently, solar power contributes approximately 11.5% of the global renewable energy share, and its contribution is expected to grow substantially in the coming decades [5]. Projections indicate that solar energy capacity may increase from nearly 2% of the renewable energy mix in 2015 to around 18% by 2040 [6]. Photovoltaic (PV) technology, in particular, offers exceptional flexibility, enabling integration into residential and commercial buildings, transportation systems, and portable electronic devices. Furthermore, large-scale solar farms have demonstrated the feasibility of harvesting solar energy on a utility scale, reinforcing its potential as a major future energy source. solar PV systems also offer strong economic advantages. Once installed, they generate electricity without fuel costs, as sunlight is freely available. This enables households, industries, and communities to reduce reliance on grid electricity and lower long-term energy expenses [7]. Additionally, PV systems can be deployed relatively quickly, especially in small- and medium-scale applications. Modular designs and standardized components allow for rapid installation and scalability, reducing the time required from project planning to power generation. The operation of photovoltaic systems is based on the photovoltaic effect, in which certain semiconductor materials generate an electric current when exposed to incident solar radiation. This direct conversion of sunlight into electrical energy forms the foundation of modern PV technology. However, a well-known limitation of PV systems is their sensitivity to operating temperature. Continuous exposure to solar radiation leads to an increase in panel temperature, which negatively affects electrical efficiency and accelerates material degradation [8]. To address this challenge, a range of cooling strategies has been proposed to regulate the operating temperature of photovoltaic (PV) panels and enhance their electrical performance. Among these approaches, passive cooling techniques are particularly attractive due to their structural simplicity, cost-effectiveness, and the absence of external energy requirements. In the present study, passive cooling methods namely phase change material (PCM) cooling, fin-based cooling, and a hybrid system combining both techniques are experimentally investigated using the configurations illustrated in **Figures 1–6**. The photovoltaic panel and its adjustable mounting arrangement are shown in **Figure 1**, while the thermal imaging instrumentation and representative surface temperature distributions are presented in **Figures 2 and 3**, respectively. The design and fabrication details of the aluminium fins are provided in **Figure 4**, and the pyranometer used for measuring incident solar irradiance is shown in **Figure 5**. The three passive cooling configurations evaluated in this study are summarized in **Figure 6**. By systematically comparing these cooling strategies under identical outdoor operating conditions, this work aims to identify an effective and practically viable solution for improving the thermal regulation and electrical performance of photovoltaic panels.

a b

Figure 1. (a) 50 W, 12 V photovoltaic panel; (b) tiltable stand used to position the photovoltaic panel.

A monocrystalline photovoltaic (PV) panel was employed in the present experimental investigation. Monocrystalline modules are fabricated from a single silicon crystal, resulting in a highly ordered and continuous lattice structure. This uniform atomic arrangement facilitates efficient charge carrier transport, leading to improved electrical performance and higher energy conversion efficiency compared with other crystalline PV technologies. The PV module used in this study is a **50 W, 12 V ANDSLITE AS-5012 monocrystalline panel**, as illustrated in **Figure 1(a)**. The key electrical and physical specifications of the PV panel are summarized as follows: the open-circuit voltage (Voc) is 22.6 V, the short-circuit current (Isc) is 2.82 A, the voltage and current at maximum power (Vmp and Imp) are 18.8 V and 2.7 A, respectively, the maximum system voltage is 1000 V, and the panel dimensions are 62 cm × 50 cm. To support and orient the PV panel during outdoor testing, a custom mounting stand was fabricated using angled iron bars, providing a rigid and stable support structure. The panel was secured to the stand using U-clamps, which also enabled convenient adjustment of the tilt angle, as shown in **Figure 1(b)**. The stand allows tilt variation from **10° to 75°**, enabling alignment of the PV panel with the sun's trajectory throughout the day. This adjustability enhances solar irradiance capture and contributes to improved energy generation. The robust construction of the mounting system ensures mechanical stability under varying environmental conditions, making it suitable for both controlled experimental studies and practical field applications.

Figure 2: Thermal camera used for measuring the temperature developed on the PV panel

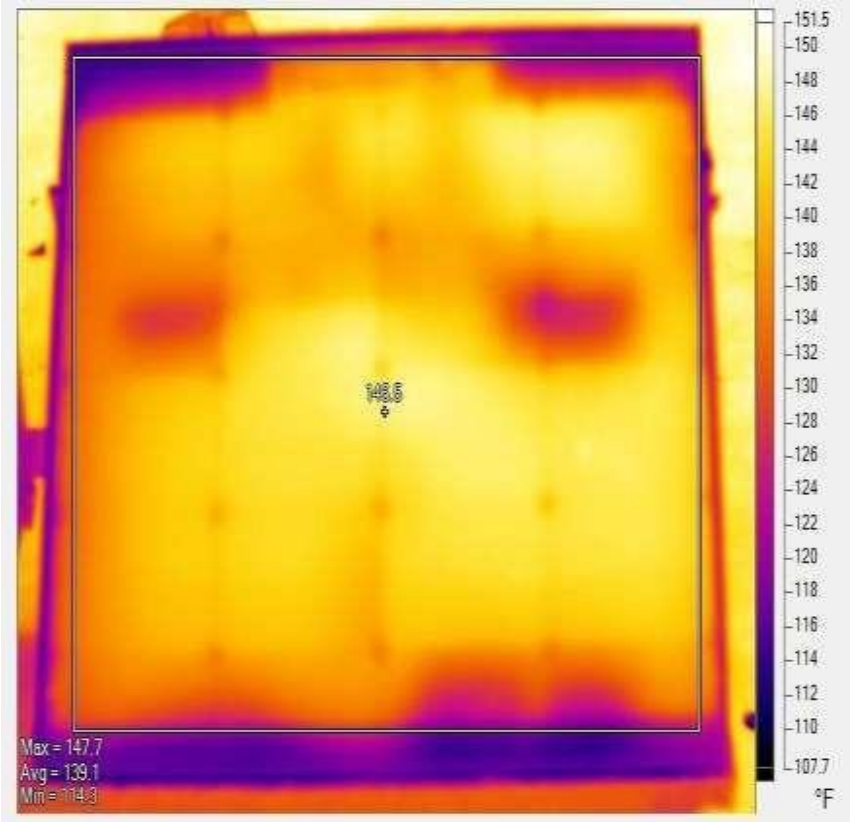

Figure 3: Sample of the thermal image

a b

Figure 4 (a) designed fins (b) Fabricated fins made up of aluminum

The L-shaped fins were designed and fabricated as a passive cooling solution to improve heat dissipation from the photovoltaic panel. Aluminium was chosen as the fin material because of its high thermal conductivity, lightweight nature, and ease of fabrication. The fin geometry and dimensions were selected based on the expected heat transfer from the PV panel, ensuring effective and reliable thermal management. The L-shaped design increases the available surface area for heat exchange, which enhances convective heat transfer to the surrounding air. The fins were arranged in a manner that allows air to flow freely through the channels between them, further improving the cooling effect. To reduce thermal resistance at the interface and ensure efficient heat conduction, a thermal paste was applied between the fins and the aluminium sheet. This helped eliminate air gaps and provided better thermal contact, resulting in improved overall cooling performance.

Figure 5: A pyranometer was used to measure the solar irradiance

A pyranometer is an actinometric instrument used to measure solar irradiance at a given location by quantifying the solar radiation flux incident on a surface. The measured irradiance is expressed in watts per square meter (W/m^2) and typically covers a broad spectral range from 300 nm to 3000 nm. Owing to its nearly flat spectral response, the pyranometer is capable of accurately capturing solar radiation across this wide wavelength range. The working principle of a pyranometer is based on sensing the temperature difference between two surfaces one dark and one transparent. The dark (black) surface of the thermopile absorbs incoming solar radiation and heats up, while the transparent surface reflects or transmits most of the radiation and therefore remains relatively cooler. This temperature difference produces an electrical signal in the thermopile, which is proportional to the intensity

of the incident solar radiation.

a b

c

Figure 6. (a) PV panel with encapsulated PCM on the rear side; (b) PV panel with fins attached on the rear side; (c) hybrid cooling system combining PCM and fins.

3. Experimental Methodology

The experimental investigation was conducted over 9 consecutive days, between **20 and 29 April**, during the time interval from **11:00 AM to 3:00 PM** each day. The experimental setup was installed in an open outdoor location free from shading or obstructions to ensure uninterrupted exposure to solar radiation. The photovoltaic (PV) panel was mounted at a fixed tilt angle of **25°**, selected based on the latitude of the experimental site to maximize incident solar irradiance. A thermal imaging camera was used to continuously monitor the surface temperature distribution of the PV panel during operation. Electrical measurements were obtained by applying a constant load using a rheostat, while the corresponding voltage and current were measured using a voltmeter and an ammeter, respectively. A pyranometer was employed to record the incident solar irradiance throughout the experimental period.

Day 1-3: PCM-Based Cooling

On the first day, passive cooling using a phase change material (PCM) was investigated. Approximately **2.5 kg of OM35 PCM**, selected based on prior numerical analysis, was applied to the rear surface of the PV panel with minimal air gap. The PCM was encapsulated and securely attached using self-adhesive aluminium tape, with additional reinforcement provided by brown tape to prevent

displacement during melting and solidification cycles. The PCM-based cooling configuration is shown in **Figure 6(a)**.

Day 4-6: Fin-Based Cooling

On the second day, **aluminium fins** were mounted on the rear surface of the PV panel to enhance heat dissipation. A thermal paste was applied at the fin–panel interface to improve thermal contact and reduce contact resistance. The fins were firmly secured using aluminium tape to ensure mechanical stability during operation. This fin-cooled configuration is illustrated in **Figure 6(b)**.

Day 7-9: Hybrid PCM–Fin Cooling

On the third day, a **hybrid cooling configuration** combining PCM and fins was implemented. The PCM was first attached to the rear surface of the PV panel following the same procedure adopted on the first day. Aluminium fins were then mounted over the PCM layer, with thermal paste applied between the fins and the PCM to eliminate air gaps and enhance heat transfer. The integration of fins was intended to improve the effective thermal conductivity of the PCM, thereby enhancing the overall cooling performance of the system. The hybrid configuration is shown in **Figure 6(c)**.

Rationale for Passive Cooling

Continuous exposure to solar radiation causes a significant rise in PV panel temperature, which adversely affects electrical efficiency and accelerates material degradation. Although both active and passive cooling techniques are available, active cooling systems generally involve higher installation costs, increased system complexity, and additional energy consumption, making them less suitable for small- and medium-scale photovoltaic installations. Passive cooling techniques, which operate without external power input, offer a simpler and more economical alternative. Among these, fin-based cooling and phase change materials have been widely investigated. However, previous studies have reported limitations related to inappropriate PCM selection or ineffective integration of multiple cooling mechanisms. This study addresses these limitations by experimentally comparing fin-based cooling, PCM-based cooling, and a hybrid cooling approach. In addition, a cost analysis is performed to identify the most economically viable cooling configuration.

Assumptions Made in the Study

- **PV Panel:** Reflection losses from the glazing surface are assumed to be 3%. Absorption of solar radiation by the glazing layer and long-wave radiation emission from the glazing surface are neglected. All transmitted solar radiation is assumed to be absorbed by the PV silicon layer. The conversion efficiency of the PV panel is expressed as a function of cell temperature, referenced to standard laboratory conditions at **25°C**.
- **PCM:** Both solid and liquid phases of the PCM are assumed to be isotropic and homogeneous. Thermophysical properties are considered constant within each phase, and no air gap is assumed between the encapsulated PCM and the rear surface of the PV panel.
- **Fins:** The thermal conductivity of the aluminium fins is assumed to be constant, and perfect thermal contact (no air gap) between the fins and the rear surface of the PV panel is assumed.

Equations Used

The electrical power output of the PV panel is calculated as:

$$P = V \times I$$

The electrical efficiency of the PV panel is given by:

$$\eta = \frac{VI}{EA} \qquad (1)$$

where
$V$is the voltage,
$I$is the current,
$E$is the solar irradiance, and
$A$is the panel area.

The **Power Enhancement Percentage (PEP)** is defined as:

$$\text{PEP } (\%) = \left(\frac{P_{\text{EXP}} - P_{\text{REF}}}{P_{\text{REF}}}\right) \times 100 \qquad (2)$$

where
$P_{\text{EXP}}$is the power output of the panel with cooling, and
$P_{\text{REF}}$is the power output of the reference panel.

The **Efficiency Enhancement Percentage (EEP)** is calculated as:

$$\text{EEP } (\%) = \left(\frac{\eta_{\text{EXP}} - \eta_{\text{REF}}}{\eta_{\text{REF}}}\right) \times 100 \qquad (3)$$

where
$\eta_{\text{EXP}}$is the efficiency of the panel with cooling, and
$\eta_{\text{REF}}$is the efficiency of the reference panel.

5. Results and Discussion

During the initial phase of the measurements, negative temperature differences were recorded in **Tables 4–6**, indicating that the reference PV panel was momentarily cooler than the panels equipped with passive cooling systems. This short-term behavior is associated with the activation dynamics of passive cooling mechanisms. At the beginning of solar exposure, both phase change materials (PCMs) and aluminum fins require a certain response time before effective heat removal can occur. Prior to the onset of PCM melting or the development of a sufficient temperature gradient to initiate natural convection along the fin surfaces, the attached cooling elements may temporarily hinder heat dissipation, behaving as weak thermal resistances. As solar irradiance increased and the PV panel temperature rose beyond the phase-change temperature range of the PCM, latent heat absorption became effective. Simultaneously, increasing air–surface temperature gradients around the fins enhanced natural convective heat transfer. Once these mechanisms were fully activated, a reversal in the temperature trend was observed, leading to a sustained reduction in panel temperature and corresponding improvements in electrical output and efficiency. A comparative assessment of PV performance under PCM-based cooling, fin-based cooling, and hybrid PCM–fin configurations relative to the uncooled reference panel is presented in **Tables 4, 5, and 6**. The results indicate that PCM integration offers moderate thermal regulation by absorbing excess heat during the phase transition period. In contrast, the aluminum fin configuration delivers the most pronounced and consistent temperature reduction, resulting in the highest improvement in electrical efficiency once steady convective cooling is established. The hybrid PCM–fin system demonstrates intermediate performance by combining latent heat storage with sensible heat dissipation; however, its effectiveness is influenced by initial thermal lag and increased

material complexity. Minor fluctuations observed in individual data points, such as brief deviations in power output or efficiency during mid-day operation, can be attributed to transient environmental effects, including intermittent cloud cover and short sensor response delays. These variations do not alter the overall performance trends. Collectively, the results provide a clear comparative understanding of the thermal behaviour of different passive cooling strategies and highlight the associated trade-offs in cooling effectiveness, efficiency enhancement, and practical feasibility.

Table 4. Reference panel vs panel with PCM

Time	Power output of the reference panel (W)	Power output of the panel cooled by using PCM	Temperature difference between the two panel	Efficiency of the reference panel (η)	Efficiency of the panel cooled by using PCM (ηpcm)
11:00	27.9	27	-2	7.9	7.7
11:15	30.38	32.928	-.88	8.8	9.55
11:30	30.38	32.928	.26	8.7	9.52
11:45	32.144	33.6	3.4	8.95	9.36
12:00	32.144	32.928	2.66	8.45	8.66
12:15	32.144	32.928	2.66	9.2	9.49
12:30	32.144	32.144	4.441	9.7	9.71
12:45	32.144	32.144	2.773	9.73	9.49
1:00	32.144	32.928	1.6	9.71	9.95
1:15	32.144	31.948	0.4	9.81	9.74
1:30	29.792	29.792	1	9.37	9.37
1:45	32.144	31.948	0.1	10.03	9.97
2:00	15.84	18.032	0	10.62	12.09
2:15	14.08	16.464	3.7	10.16	11.88

Table 5. Reference panel vs panel with fins

Time	Power output of the reference panel	Power output of the panel cooled by using fins	Temperature difference between the two panel	Efficiency of the reference panel (η)	Efficiency of the panel cooled by using fins (ηfins)
11:00	29.30	29.30	-0.1	12.9	12.8
11:15	27.36	26.6	-0.51	12	13
11:30	27.36	28.992	0	11.1	11.8
11:45	27.36	28.992	5.66	13.2	13.2
12:00	14.96	15.84	4.72	7.2	10.33
12:15	27.44	28.22	0.82	12.5	9.76
12:30	27.44	29.53	0.5	8.5	10.3

12:45	27.44	29.53	7.98	8.66	13.5
1:00	27.44	29.55	10	8.2	9.3
1:15	27.44	29.4	10.37	8.69	9.3
1:30	28.22	29.4	2.95	9.2	9.5
1:45	27.44	29.4	2.91	9.1	9.8
2:00	27.44	29.4	5.39	9.3	9.9
2:15	27.44	29.4	1.55	8.8	9.4
2:30	27.44	29.4	2.73	10.1	10.8
2:45	27.44	29.4	0.77	9.9	10.7
3:00	26.656	28.71	2.22	10.3	11.11

Table 6. Reference panel vs panel with hybrid combination of fins and PCM

Time	**Power output of the reference panel**	**Power output of the panel cooled by using hybrid PCM-fins**	**Temperature difference between the two panel**	**Efficiency of the reference panel (η)**	**Efficiency of the panel cooled by using hybrid PCM-fins (ηpcm-fins)**
11:00	29.1	29.55	0.5	9.09	9.24
11:15	29.1	29.55	-1.3	9.98	10.1
11:30	29.1	31.4	0.1	8	8.6
11:45	23.852	25.56	1.66	6.59	7.06
12:00	26.864	29.4	5.5	7.27	8.7
12:15	26.864	29.4	2	7.35	8.05
12:30	26.864	29.4	1.62	7.23	8.64
12:45	27.6	29.4	1.4	7.6	8.1
1:00	26.864	29.4	0.09	7.42	8.12
1:15	26.864	29.4	1.3	7.97	8.72
1:30	26.128	28.8	2.4	8.4	8.97
1:45	26.128	28.5	1.63	8.5	9.54
2:00	26.128	28.324	2.7	8.38	9.08
2:15	26.128	28.324	1.4	8.86	9.6
2:30	26.864	28.324	2.1	8.73	9.22
2:45	26.864	28.324	0.5	9.41	9.97
3:00	26.128	28.324	0.6	9.28	10.06

5.1. Panel with PCM

The photovoltaic panel equipped with a phase change material (PCM) demonstrated a noticeable improvement in electrical power output compared with the uncooled reference panel once thermal activation was achieved. The time-dependent variation in power output for the PCM-cooled configuration is illustrated in **Figure 7**. During the initial period of solar exposure, the reference panel generated slightly higher power than the PCM-integrated panel. This behaviour can be explained by the delayed thermal response of the PCM, which had not yet reached its phase-transition temperature and therefore remained inactive in terms of latent heat absorption. At this stage, the PCM layer functioned primarily as a thermal mass rather than an effective cooling medium. As solar irradiance increased and the operating temperature of the PV panel rose, the PCM entered its melting range, activating latent heat storage and lowering the panel temperature. This thermal regulation translated into enhanced electrical performance, with the largest power difference occurring at approximately **11:30 AM**, when the PCM-cooled panel achieved a maximum power output of **32.93 W**. After around **1:15 PM**, the power outputs of the cooled and reference panels began to converge, indicating partial saturation of the PCM and a diminishing capacity for additional heat absorption under prolonged thermal loading. Across the entire experimental duration, the PCM-based cooling configuration yielded an average power enhancement of **3.02%** relative to the reference panel. These findings suggest that PCM integration offers a moderate and time-dependent improvement in PV performance, with the most significant benefits observed during mid-day operation when panel temperatures exceed the PCM phase-change threshold. Although the level of enhancement is lower than that obtained with fin-assisted cooling, the PCM system provides passive thermal buffering without dependence on ambient airflow, making it particularly suitable for environments where natural convection is limited.

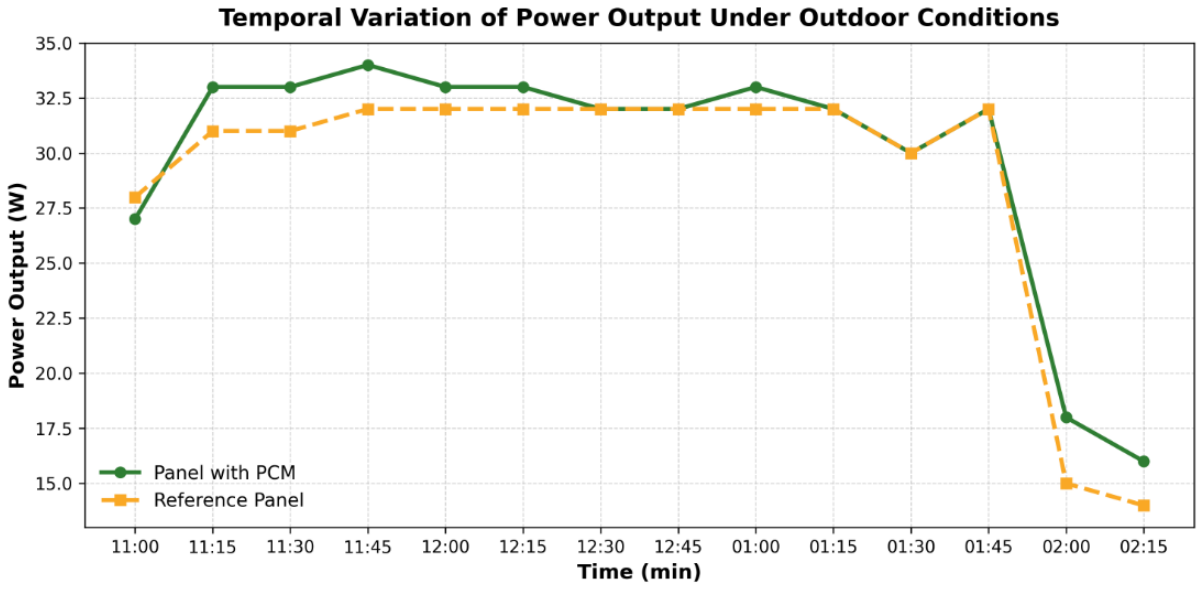

Figure 7. Time vs Power graph (panel with PCM-Reference panel)

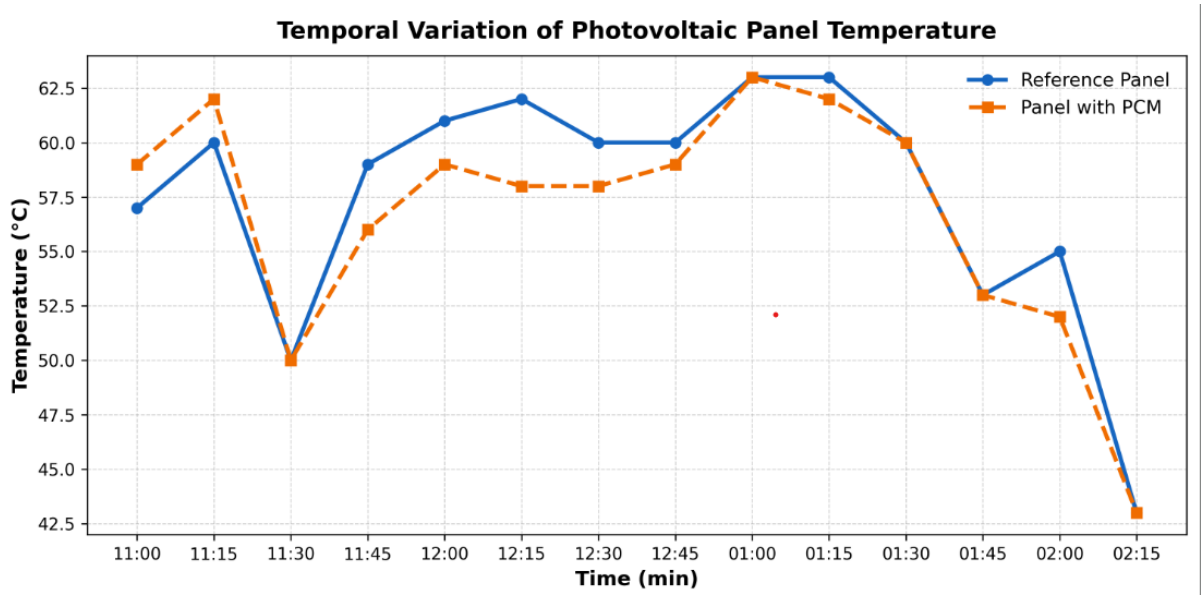

Figure 8. Time vs Temperature graph (panel with PCM Vs reference panel)

Figure 8 presents the temporal variation of surface temperature for the PCM-cooled photovoltaic panel and the uncooled reference panel. During the initial stage of exposure, the PCM-integrated panel exhibited a slightly higher surface temperature than the reference panel. This behaviour is attributed to the thermal inertia of the PCM, which had not yet reached its phase-transition temperature and therefore did not actively absorb latent heat. As solar irradiance increased and the panel temperature approached the PCM melting range, a gradual reduction in surface temperature was observed for the PCM-cooled configuration. The maximum temperature difference between the two panels reached **4.44 °C** at approximately **12:30 PM**, indicating effective thermal energy absorption during peak irradiance conditions. Beyond this period, the temperature difference diminished as the PCM approached thermal saturation under sustained heating. These results confirm that PCM-based cooling provides a time-dependent thermal buffering effect, with the greatest temperature reduction occurring once the phase change process is fully activated.

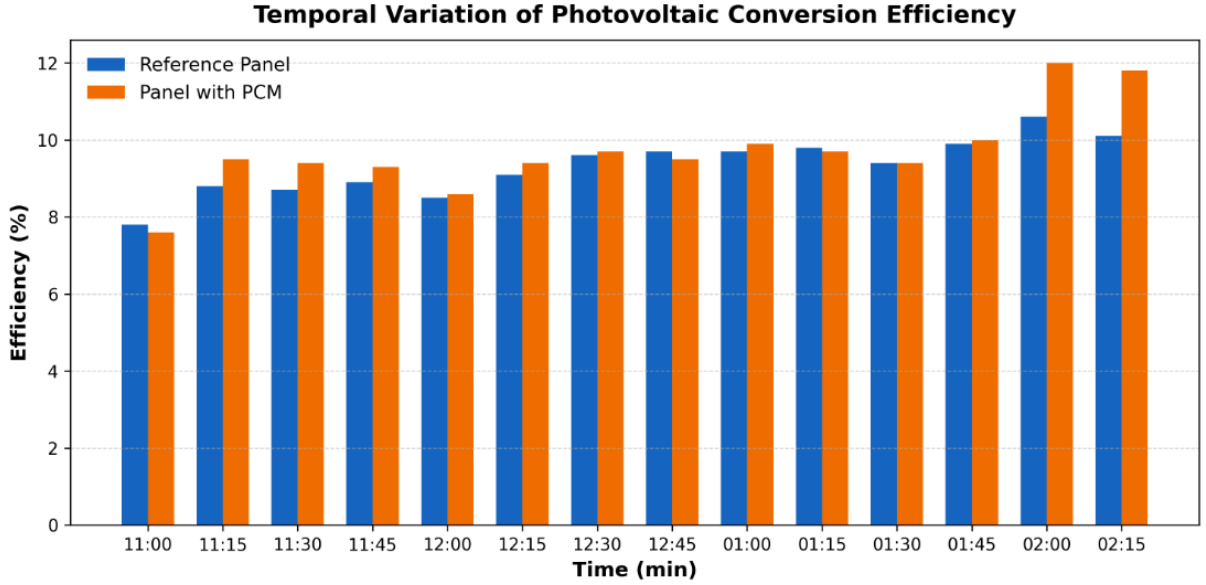

Figure 9. Time vs Efficiency (panel with PCM- reference panel)

The time–efficiency profile shown in Figure 9 indicates that the integration of phase change material (PCM) resulted in a modest but consistent improvement in the electrical efficiency of the photovoltaic panel once thermal activation occurred. Over the full measurement period, the PCM-cooled configuration achieved an average efficiency enhancement of **4.48%** relative to the uncooled reference panel. This improvement is primarily associated with the reduction in operating temperature during peak irradiance hours, confirming the role of latent heat absorption in mitigating temperature-induced efficiency losses.

5.2. Panel with fins

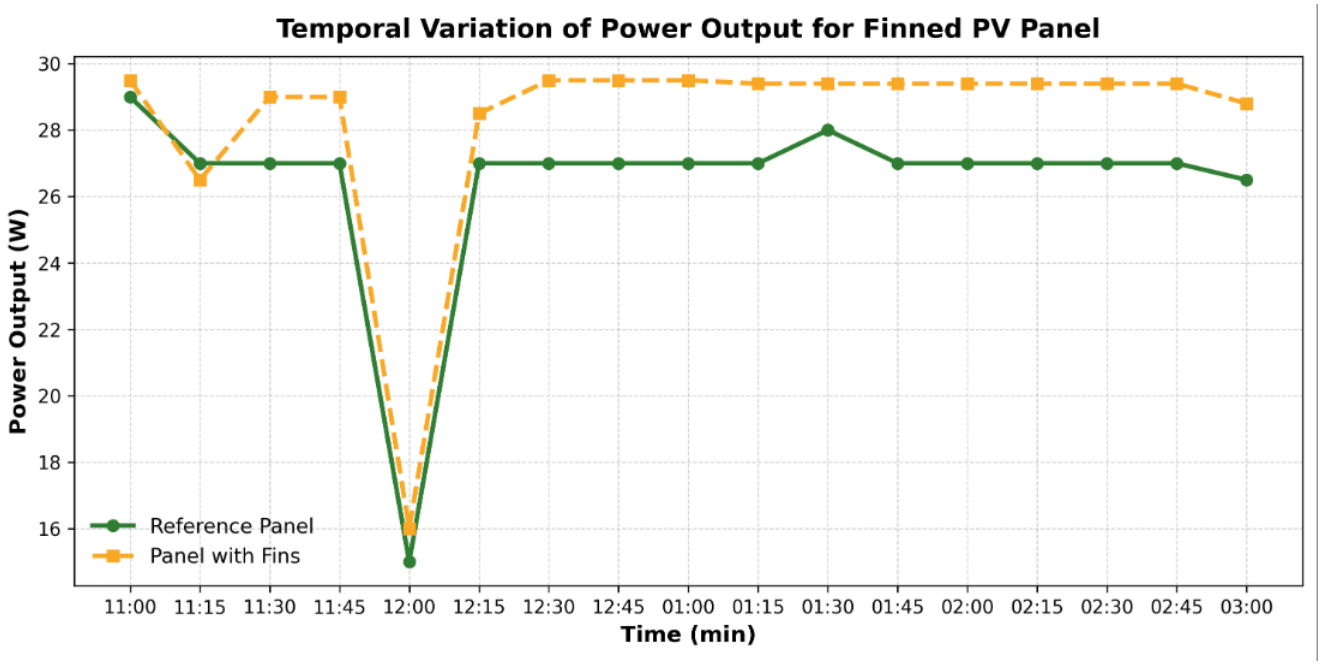

Figure 10. Time vs power graph (panel with fins vs reference panel)

Figure 10 shows the temporal variation in power output for the photovoltaic panel equipped with aluminium fins compared with the uncooled reference panel. Once natural convection was fully established, the fin-cooled panel consistently produced higher electrical power than the reference configuration. This improvement is attributed to enhanced convective heat dissipation from the rear surface of the panel, which reduced operating temperature and mitigated temperature-induced voltage losses. A maximum power output of **29.55 W** was recorded at approximately **1:00 PM**, corresponding to a **5.55% increase** relative to the uncooled panel. This result demonstrates the effectiveness of extended-surface cooling in sustaining electrical performance during periods of high solar irradiance. Figure 11 illustrates the corresponding surface temperature variation for the fin-cooled and reference panels. Among the cooling strategies investigated, the aluminium fin configuration achieved the largest temperature reduction. The increased effective surface area provided by the fins promoted natural convective heat transfer, leading to superior thermal regulation once convection stabilized. The maximum temperature difference observed was **10.37 °C** at approximately **1:15 PM**, confirming the strong cooling capability of the fin-based system under peak thermal loading conditions.

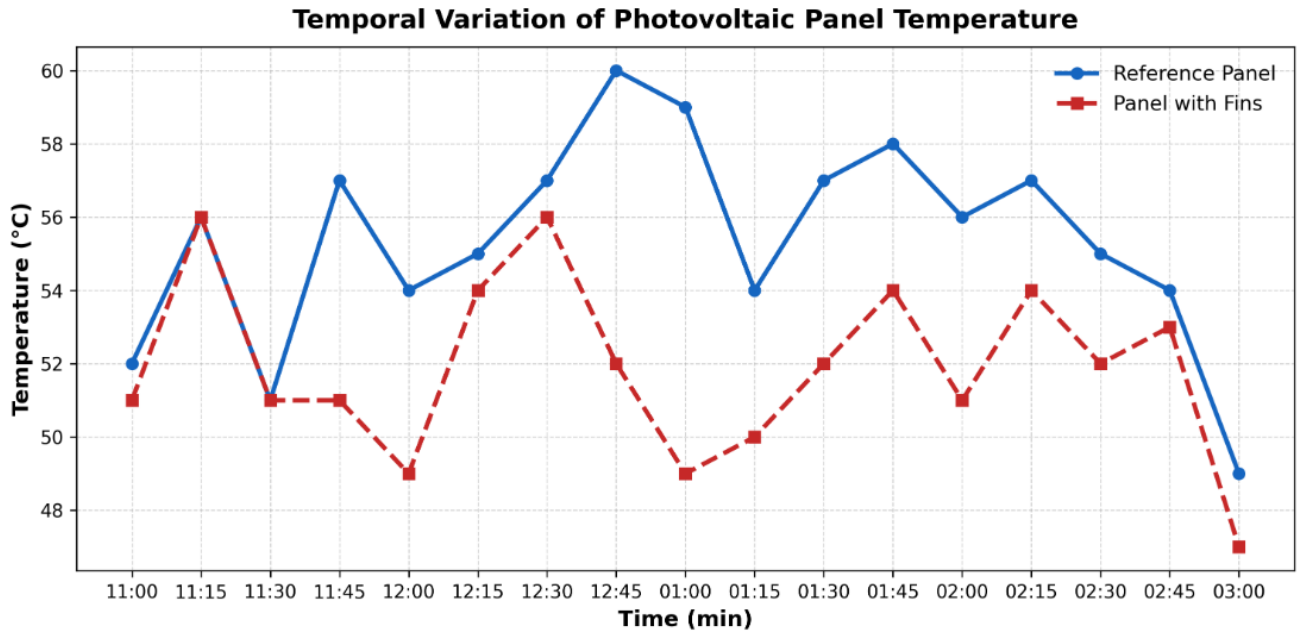

Figure 11. Time vs Temperature graph (panel with fins Vs reference panel)

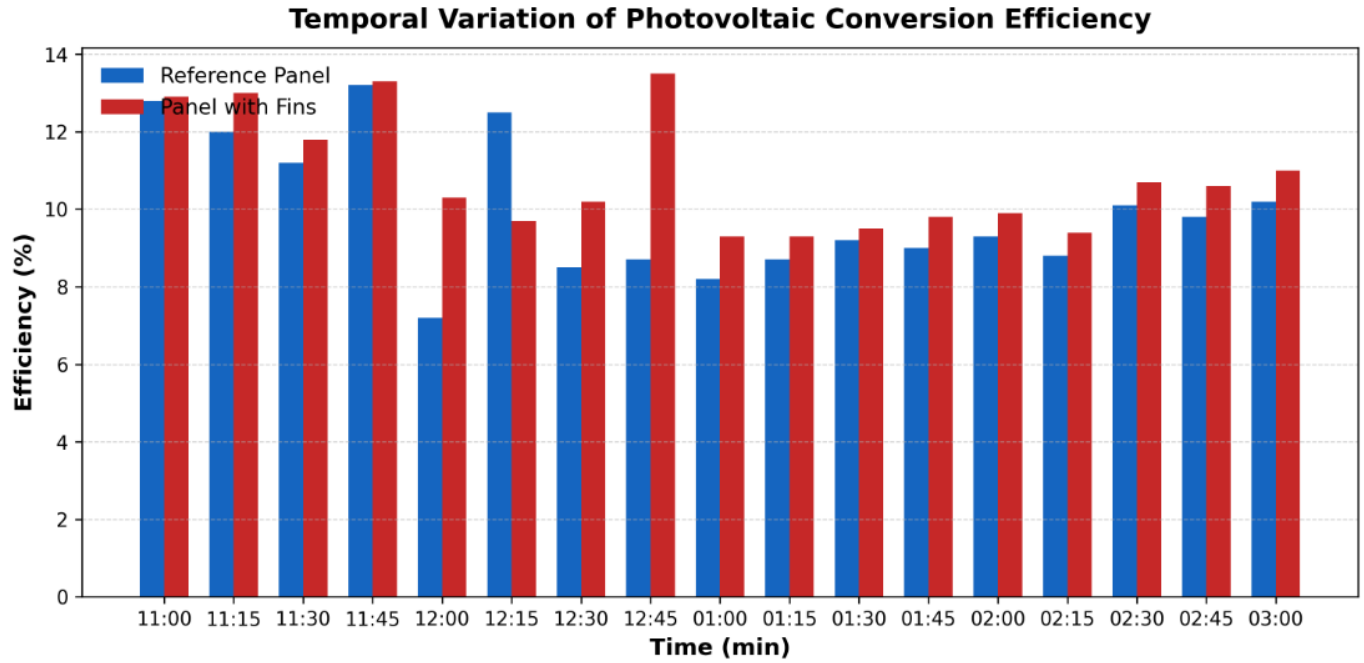

Figure 12. Time vs Efficiency graph (panel with fins Vs reference panel)

Figure 12 illustrates that the incorporation of aluminum fins significantly enhanced the efficiency of the photovoltaic panel. The fin-cooled configuration achieved a peak efficiency of 13.2%, representing an 8.85% improvement over the uncooled reference system.

5.3. Panel with hybrid system.

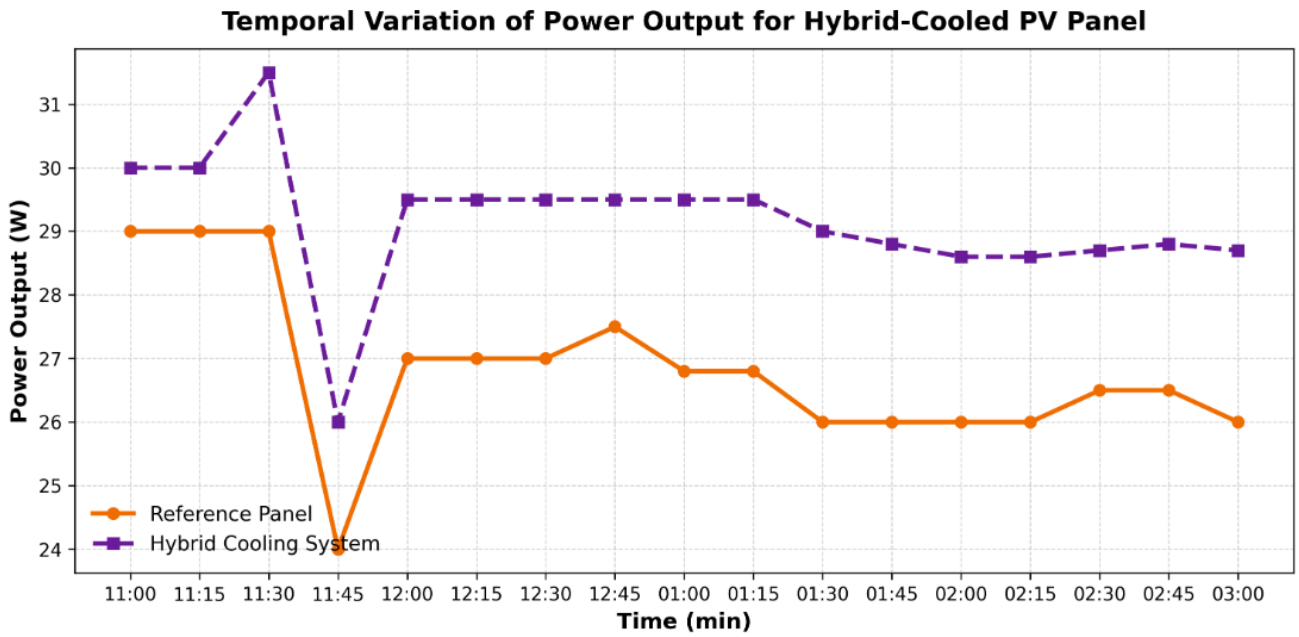

Figure 13. Time vs Power graph (panel with hybrid system Vs reference panel)

Figure 13 presents the temporal variation in power output for the hybrid PCM–fin cooling configuration compared with the uncooled reference panel. The hybrid system produced higher electrical power than the reference panel during most of the test period, with a maximum output of **31.4 W** observed at approximately **11:30 AM**. Despite this improvement, the overall power enhancement was limited to **7.57%**, which was lower than that achieved by the fin-only configuration. This behaviour can be attributed to the presence of the PCM layer between the photovoltaic panel and the fins. While the PCM contributes to latent heat absorption during phase transition, its relatively low thermal conductivity introduces an additional conduction resistance that partially impedes heat transfer from the panel to the fins. As a result, the effectiveness of convective heat dissipation is reduced once the PCM approaches thermal saturation, leading to diminished overall cooling performance compared with direct fin–panel contact. These results indicate that hybrid PCM–fin systems offer a balanced but time-dependent cooling response, combining latent heat buffering with convective dissipation. However, the added thermal resistance and material cost must be carefully considered when evaluating hybrid designs for practical photovoltaic applications.

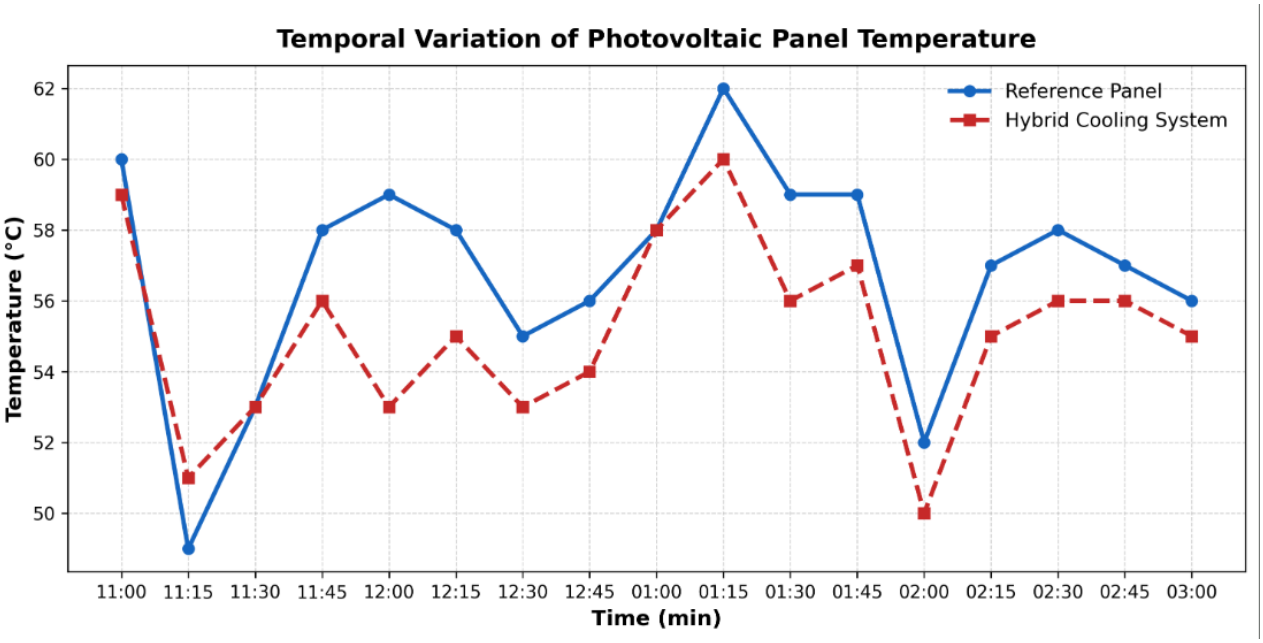

Figure 14. Time vs Temperature (panel with hybrid system Vs reference panel)

Although the hybrid PCM–fin configuration reduced the surface temperature of the photovoltaic panel relative to the uncooled reference, its thermal performance remained lower than that of the standalone fin system, as shown in Figure 14. This behaviour arises from the additional thermal resistance introduced by the PCM layer positioned between the panel and the fins. While the PCM contributes to latent heat absorption during phase transition, its comparatively low thermal conductivity limits heat transfer to the fins, thereby reducing the effectiveness of convective cooling. As a result, the hybrid system exhibits a moderated cooling response, particularly once the PCM approaches thermal saturation under sustained irradiance. The maximum temperature difference between the hybrid-cooled and reference panels was **5.5 °C**, recorded at approximately **12:00 PM**, confirming partial thermal regulation but highlighting the trade-off between latent heat buffering and convective heat dissipation in hybrid designs.

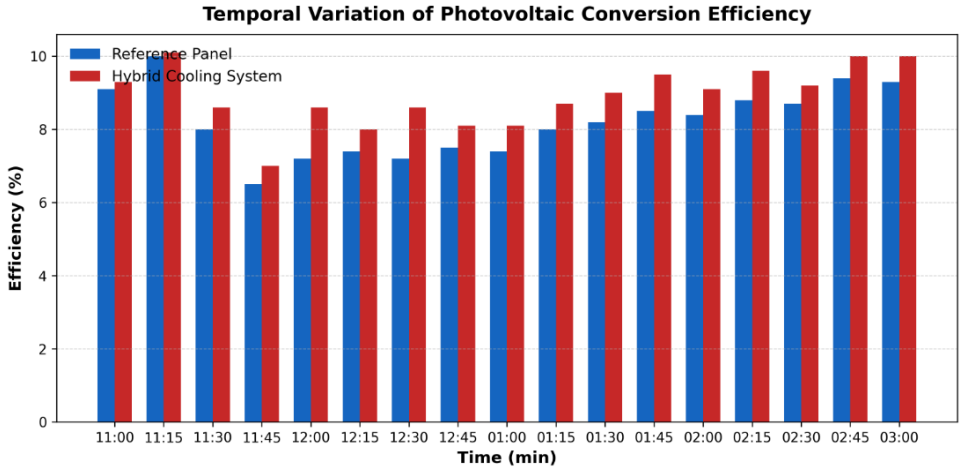

Figure 15. Time vs Efficiency graph (panel with hybrid system Vs reference panel)

Figure 15 shows that the hybrid PCM–fin cooling configuration resulted in a measurable improvement in the electrical efficiency of the photovoltaic panel compared with the uncooled reference. The maximum efficiency recorded for the hybrid system was **10.1%**, corresponding to an average efficiency enhancement of **7.8%**. This

improvement reflects the combined contribution of latent heat absorption by the PCM and convective heat dissipation through the fins. However, as discussed earlier, the overall efficiency gain remains lower than that achieved by the fin-only configuration due to the additional thermal resistance introduced by the PCM layer, which limits heat transfer to the fins under sustained operating conditions.

5. Conclusions

This study experimentally investigated the effectiveness of three passive cooling strategies fin-based cooling, phase change material (PCM) cooling, and a hybrid system combining fins and PCM for improving the thermal and electrical performance of photovoltaic (PV) panels. The experimental results confirm that all three cooling approaches effectively reduced the operating temperature of the PV module, leading to measurable improvements in power output, electrical efficiency, and a potential extension of panel service life. Among the cooling methods evaluated, the fin-assisted configuration demonstrated the best overall performance, achieving the highest temperature reduction of approximately **10.37 °C**. This substantial decrease in operating temperature translated into a pronounced enhancement in PV electrical performance. In comparison, the hybrid PCM–fin system and the standalone PCM configuration resulted in temperature reductions of **5.5 °C** and **4.4 °C**, respectively. While PCM-based cooling proved effective during the phase-transition process, its cooling capacity diminished after complete melting of the material. The hybrid configuration did not deliver the expected performance improvement, which can be attributed to the relatively low thermal conductivity of the PCM and possible thermal resistance at the PCM–fin interface, limiting effective heat transfer. The study also emphasizes the influence of thermal cycling repeated heating during daytime operation followed by cooling at night on the long-term degradation of PV panels. By mitigating temperature fluctuations, passive cooling strategies can reduce thermal stresses and contribute to improved durability and long-term performance of photovoltaic modules. Overall, the findings strongly indicate that fin-based passive cooling offers a simple, effective, and economically viable solution for enhancing the performance of PV panels. Although the results are specific to the experimental conditions considered in this study including the selected PV module, OM35 phase change material, and the measurement setup employing a digital voltmeter, ammeter, and rheostat they provide valuable insights and a solid foundation for further research. Future investigations under different climatic conditions, PV technologies, and PCM formulations are recommended to validate and extend the applicability of passive cooling techniques for real-world photovoltaic systems.

Declaration

This manuscript represents the author's corrected version of a paper previously published in *International Journal of Scientific Development and Research (IJSDR)* in May 2025. Only minor typographical and formatting corrections have been made; the scientific content, data, results, and conclusions remain unchanged. The published version of record is available at: https://doi.org/10.56975/ijsdr.v10i4.302395.

Conflict of Interest

The authors declare no conflict of interest.

References

1. Bayrak, F., Oztop, H. F., & Selimefendigil, F. (2020). Experimental study for the application of different

cooling techniques in photovoltaic (PV) panels. Energy Conversion and Management, 212, 112789. https://doi.org/10.1016/j.enconman.2020.112789

2. Jobair, H. K. (2017). Improving of photovoltaic cell performance by cooling using two different types of fins. International Journal of Computer Applications, 157(5), 6–15. https://doi.org/10.5120/ijca2017912691
3. Sharaf, M., Yousef, M. S., & Huzayyin, A. S. (2022). Review of cooling techniques used to enhance the efficiency of photovoltaic power systems. Environmental Science and Pollution Research, 29(18), 26131–26159. https://doi.org/10.1007/s11356-022-18719-9
4. Hasan, A., McCormack, S. J., Huang, M. J., & Norton, B. (2014). Characterization of phase change materials for thermal control of photovoltaics using differential scanning calorimetry and temperature history method. Energy Conversion and Management, 81, 322–329. https://doi.org/10.1016/j.enconman.2014.02.042
5. Karthick, A., Murugavel, K. K., Kumaresan, G., & Sudhakar, K. (2020). Investigation of inorganic phase change material for a semi-transparent photovoltaic (STPV) module. Energies, 13(14), 3582. https://doi.org/10.3390/en13143582
6. Sutanto, B., Maulana, M. I., Saputra, Y. R., & Nugroho, A. (2022). Enhancing the performance of floating photovoltaic system by using thermosiphon cooling method: Numerical and experimental analyses. International Journal of Thermal Sciences, 180, 107727. https://doi.org/10.1016/j.ijthermalsci.2022.107727
7. Fouad, M. M., Shihata, L. A., & Morgan, E. I. (2017). An integrated review of factors influencing the performance of photovoltaic panels. Renewable and Sustainable Energy Reviews, 80, 1499–1511. https://doi.org/10.1016/j.rser.2017.05.141
8. Bahaidarah, H. M. S., Baloch, A. A. B., & Gandhidasan, P. (2016). Uniform cooling of photovoltaic panels: A review. Renewable and Sustainable Energy Reviews, 57, 1520–1544. https://doi.org/10.1016/j.rser.2015.12.064
9. Grubišić-Čabo, F., Nižetić, S., & Marco, T. G. (2016). Photovoltaic panels: A review of the cooling techniques. Transactions of FAMENA, 40(SI-1), 63–74. https://doi.org/10.21278/TOF.40201
10. Moharram, K. A., Abd-Elhady, M. S., Kandil, H. A., & El-Sherif, H. (2013). Enhancing the performance of photovoltaic panels by water cooling. Ain Shams Engineering Journal, 4(4), 869–877. https://doi.org/10.1016/j.asej.2013.03.005
11. Belsky, A. A., Dobrotvorskiy, M. A., Tatarintsev, A. A., & Yurchenko, A. V. (2022). Analysis of specifications of solar photovoltaic panels. Renewable and Sustainable Energy Reviews, 159, 112239. https://doi.org/10.1016/j.rser.2022.112239
12. Gerbinet, S., Belboom, S., & Léonard, A. (2014). Life cycle analysis (LCA) of photovoltaic panels: A review. Renewable and Sustainable Energy Reviews, 38, 747–753. https://doi.org/10.1016/j.rser.2014.07.043
13. Weckend, S., Wade, A., & Heath, G. A. (2016). End of life management: Solar photovoltaic panels (NREL/TP-6A20-73852). National Renewable Energy Laboratory. https://doi.org/10.2172/1561525
14. Rehman, S., Bader, M. A., & Al-Moallem, S. A. (2007). Cost of solar energy generated using photovoltaic panels. Renewable and Sustainable Energy Reviews, 11(8), 1843–1857. https://doi.org/10.1016/j.rser.2006.03.005